Geochemical Journal, Vol. 52, pp. e29 to e38, 2018 doi:10.2343/geochemj.2.0545

EXPRESS LETTER

Organic complexation of zinc in a coastal hydrothermal area, Tachibana Bay, Nagasaki, Japan

TAEJIN KIM,[1,2]* HAJIME OBATA,[1] SHIGENOBU TAKEDA,[3] KUO HONG WONG,[1]
ASAMI SUZUKI MASHIO[1,4] and TOSHITAKA GAMO[1]

[1]Atmosphere and Ocean Research Institute, The University of Tokyo, 5-1-5 Kashiwanoha, Kashiwa, Chiba 277-8564, Japan
[2]School of Earth and Environmental Sciences, Seoul National University,
1 Gwanak-ro, Gwanak-gu, Seoul 08826, Republic of Korea
[3]Graduate School of Fisheries and Environmental Sciences, Nagasaki University, 1-14 Bunkyo-machi, Nagasaki 852-8521, Japan
[4]College of Science and Technology, Kanazawa University, Kakuma, Kanazawa, Ishikawa 920-1192, Japan

(*Received August 23, 2018; Accepted October 22, 2018; Online published November 12, 2018*)

Distributions of trace metals (Mn, Fe, Cu, and Zn) and Zn chemical speciation were determined in Tachibana Bay to investigate the role of organic complexing ligands and sulfide on Zn in a coastal hydrothermal system. At the coastal area near Obama Hot Springs, dissolved sulfide was only detected in two bottom water samples in Stn. 6 (29.2 and 59.4 nM). At this coastal area, dissolved Mn and Fe concentrations were high and increased toward the bottom, whereas dissolved Cu and Zn concentrations generally decreased toward the bottom. The Zn complexing organic ligands (C_L) and conditional stability constants (log $K'_{ZnL,Zn2+}$) in Tachibana Bay ranged from 0.9 nM to 1.6 nM and from 9.9 to 10.3, respectively. The free sulfide concentration calculated from Zn chemical speciation was much lower than the measured dissolved sulfide concentrations. Although dissolved Zn mainly precipitate as sulfide in shallow hydrothermally active area, the organic complexation of Zn is important in the remaining dissolved Zn.

Keywords: shallow hydrothermal system, Tachibana Bay, dissolved trace metals, zinc speciation, sulfide

Abbreviations: APDC, ammonium 1-pyrrolidinedithiocarbamate; CA, carbonic anhydrase; CLE-ACSV, competitive ligand equilibrium/adsorptive cathodic stripping voltammetry; CSV, cathodic stripping voltammetry; CTD, conductivity, temperature, depth; ICP-MS, inductively coupled plasma mass spectrometry; LDPE, low-density polyethylene; PIPES, piperazine-1,4-bis (2-ethanesulfonic acid); UV, ultraviolet; UVSW, UV-irradiated seawater; Zn-PDC, Zn complexed with APDC

INTRODUCTION

Trace metals in seawater play important roles in controlling the growth of many marine microorganisms. Zinc (Zn), in particular, is used in numerous enzyme systems involved with a variety of metabolic processes and low Zn concentrations in surface seawater can limit the growth of some types of phytoplankton (e.g., Morel and Price, 2003).

It has been widely recognized that rivers and atmospheric dust depositions are the major sources of dissolved Zn to the ocean. Hydrothermally derived dissolved Zn has not been considered to be a major player in the oceanic Zn cycle because a large portion of the metal sulfides in hydrothermal fluid precipitates onto the seafloor in the direct vicinity of the hydrothermal vent and is mostly removed within a few meters above the vent (e.g., German *et al*., 1991). However, previous studies focusing on dissolved Fe and Cu in hydrothermal systems have suggested the formation of Fe- and Cu-sulfide nanoparticles in hydrothermal plumes (Sands *et al*., 2012 and reference therein), complexation by organic ligands (Sander and Koschinsky, 2011), and reversible exchange onto organic particles (Fitzsimmons *et al*., 2017) that prevents dissolved Fe and Cu from precipitating or settling gravitationally. Recently, dissolved Zn enrichments near hydrothermal vents in the deep open ocean have also been observed (e.g., Roshan *et al*., 2016), which suggests that mantle-derived Zn from hydrothermal vents could be a major source of dissolved Zn in the ocean environment (Roshan *et al*., 2016). Sander and Koschinsky (2011) stated that organic ligands potentially could stabilize dissolved Zn in hydrothermal fluids and plumes, which would increase the Zn flux to the open ocean similarly to

*Corresponding author (e-mail: tkim0206@snu.ac.kr)

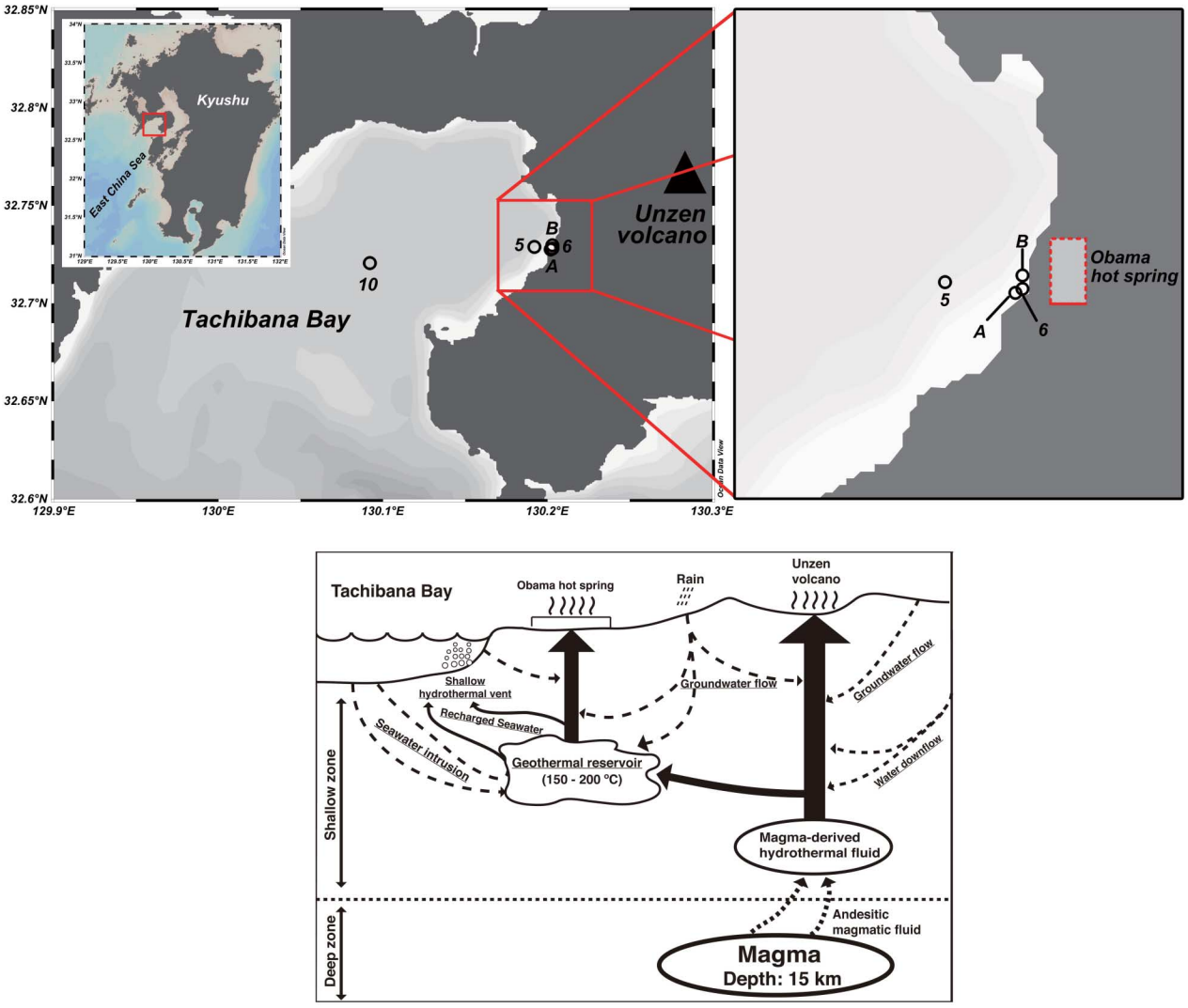

Fig. 1. (Top) Location of sampling sites in Tachibana Bay. (Bottom) Simplified conceptual model of shallow hydrothermal activity area, Tachibana Bay (modified from Saibi and Ehara, 2010; Takeda, 2018).

the case of Fe and Cu. However, this process in the hydrothermal system has not been investigated sufficiently.

Tachibana Bay is located adjacent to the Shimabara Peninsula, west of Unzen volcano located at the western part of Kyushu Island, southwestern Japan (Fig. 1). Non-buoyant hydrothermal activity has been reported in Tachibana Bay at the coastal area near Obama Hot Springs on land (Takeda, 2018 and reference therein). Previous studies have suggested that seawater is intruded into the hydrothermal system in Tachibana Bay, which is located between 200 and 620 m below sea level, and then heated in the geothermal reservoir (150–200°C). Altered seawater (pH 6.0–8.7), which is mixed with groundwater in the geothermal reservoir, is discharged with gas bubbles into the coastal area of Tachibana Bay near the Obama Hot Springs via many small holes (~1 cm diameter) on the surface of the bottom sediment (Saibi and Ehara, 2010; Takeda, 2018) (Fig. 1). Furthermore, dark subsurface sediment with a different elemental composition characterized by higher contents of Fe, S, Sb, and As has been observed at the hydrothermally active region (Takeda, 2018).

In this study area, we determined dissolved trace metal (Mn, Fe, Cu, and Zn) concentrations, Zn speciation, and dissolved sulfide in seawater. We focused on the Zn complexing organic ligands in Tachibana Bay, to investigate the roles of organic complexing ligands and sulfide on Zn in the coastal hydrothermal system.

Materials and Methods

Sampling location and method

Seawater samples were collected at five sampling sites during a research cruise KY-340 of TS *Kakuyo-maru* in May 2012 (Fig. 1). In Tachibana Bay, three sites (Stn. A, Stn. B, and Stn. 6) were located at coastal areas near the Obama Hot Springs on land, where the hydrothermal activity was reported previously (Takeda, 2018), and the other two sites (Stn. 5 and Stn. 10) were located slightly away from the coastal area and at the center of the bay, respectively. Prior to the seawater sampling, we confirmed the hydrothermal activities by the observations of fumarolic gas emissions using quantitative echosounder (FQ-80, Furuno) near the coast of Obama Hot Springs (Supplementary Fig. S1), which was reported previously (Takeda, 2018). The seawater samples were collected by acid-cleaned 5-L OTE (Ocean Test Equipment) samplers with external springs mounted on a SeaBird conductivity, temperature, depth (CTD) carousel array suspended from the vessel by a stainless steel-armored cable. The seawater samples were filtered immediately using an acid-cleaned 0.2-μm Acropak filter cartridge (PALL Co.) directly connected to the OTE sampler spigot. Firstly, samples used for dissolved sulfide measurement were collected into a polypropylene syringe through the polyethylene tube through a 3-way valve not to expose to the air. Then, dissolved sulfide concentrations were determined immediately in the onboard laboratory of the research vessel. Samples for dissolved trace metals and Zn speciation measurements were collected in acid-cleaned 500-mL low-density polyethylene (LDPE) bottles (Nalgene/Thermo Fisher) after rinsing three times with filtered seawater.

The samples for measurement of dissolved trace metal concentrations were acidified to pH < 1.8 by using ultrapure HCl (Tamapure AA-100, Tama Chemicals) and then stored. The filtered samples for Zn speciation measurements were frozen immediately after collection and maintained until their analysis. The samples for dissolved trace metals and Zn speciation determination were analyzed at the Atmosphere and Ocean Research Institute, The University of Tokyo.

Analyses of dissolved Mn, Fe, and Cu in seawater

Dissolved Mn, Fe, and Cu concentrations were determined using a chelating resin (Nobias Chelate-PA1, Hitachi High Technologies) preconcentration and inductively coupled plasma mass spectrometry (ICP-MS) method (Kondo *et al*., 2016). Acidified seawater sample (10 mL) was directly introduced into the column with a peristaltic pump. After the seawater sample was loaded, 17.5 mL of 0.05 M ammonium acetate buffer solution (for pH 6.0), which was prepared by mixing NH_4OH (Tamapure AA-100, Tama Chemicals) and glacial acetic acid (Optima, Fisher Chemical), was passed through the column to remove sea salts in the column. The trace metals were then eluted with 5 mL of 1 M HNO_3 (Tamapure AA-100, Tama Chemicals) from opposite direction of sample loading using a Teflon syringe. The system used for this study had four parallel lines and could process four samples simultaneously (Kondo *et al*., 2016). The concentrations of dissolved Mn, Fe, and Cu in the eluent were determined with a Thermo Scientific ELEMENT XR mass spectrometer using the medium resolution mode; a calibration curve method was applied using a diluted metal standard solution (ICP-MS Multi-Element Solution, 100 mg/L, SPEX) prepared in 1 M HNO_3 with concentration ranges of 1.8–36.4 nM, 1.8–35.8 nM, and 1.6–31.5 nM for Mn, Fe, and Cu, respectively. For this study, the detection limits, defined as three times the standard deviation of the blank measurements (n = 4), for Mn, Fe, and Cu were 0.003 nM, 0.061 nM, and 0.014 nM, respectively. The GEOTRACES standard seawater samples, which were collected by trace metal clean sampling method for world-wide analytical intercomparisons (www.geotraces.org), GD (n = 2) and SAFe D2 (n = 2) were run as quality control checks for the data, and the results agreed well with the reported consensus values (Supplementary Table S1).

Analysis of dissolved Zn in seawater

Cathodic stripping voltammetry (CSV) was used to determine dissolved Zn concentrations in the seawater (Kim *et al*., 2015). We used a 757 VA Computrace (Metrohm) voltammetric system. The seawater samples were UV-irradiated for 40 min and readjusted to pH 7.0 with aqueous ammonia and buffer solution of piperazine-1,4-bis(2-ethanesulfonic acid) (PIPES) just before the analyses. The concentrations of Zn in the seawater were calculated using a standard addition method. The procedural blank value was obtained from Zn-removed seawater that had been passed through a chelating resin column (Nobias Chelate-PA1, Hitachi High Technology). This Zn-free seawater was irradiated with an UV lamp to decompose the artificial ligand, which originated from the chelating resin column (Kim *et al*., 2015). The resulting procedural blank value was calculated as 81 ± 6 pM (n = 7). This blank value was subtracted from the measured values to calculate the dissolved Zn concentrations. The detection limit, defined as three times the standard deviation of the Zn-free seawater measurements, was 18 pM. To assess the accuracy of the entire analytical procedure, Zn concentrations were determined in GEOTRACES GS (n = 3) and GD (n = 3) and compared. The results of this intercalibration agreed well with the reported consensus values (Table S1).

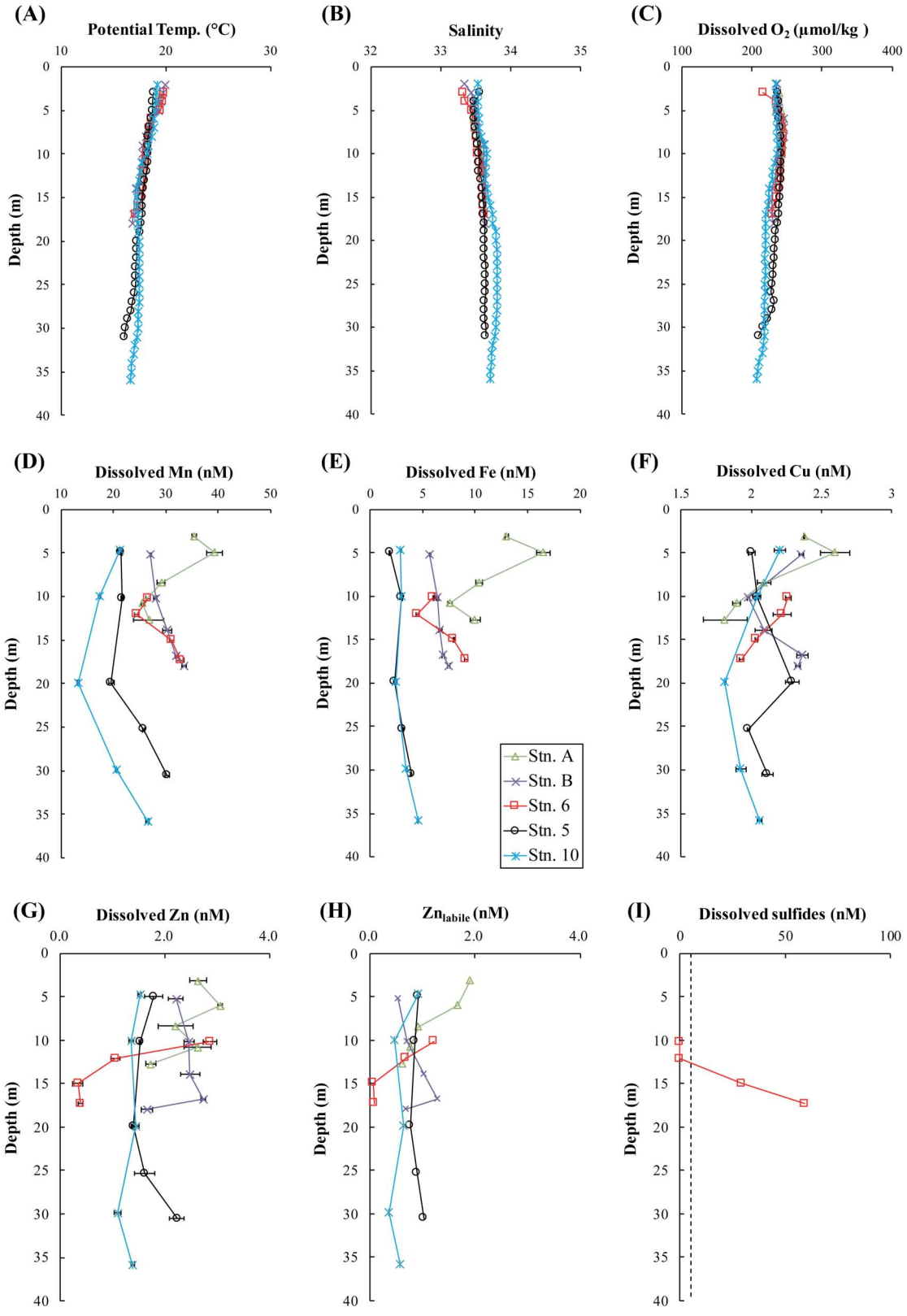

Fig. 2. Vertical distributions of (A) potential temperature, (B) salinity, (C) dissolved oxygen, (D) dissolved Mn, (E) dissolved Fe, (F) dissolved Cu, (G) dissolved Zn, (H) Zn_{labile}, and (I) dissolved sulfides in Tachibana Bay. Black dotted line in vertical distribution of dissolved sulfides indicates detection limit of CSV method (4.8 nM).

Zn speciation analysis

Zn speciation was determined through titration by using competitive ligand equilibrium/adsorptive cathodic stripping voltammetry (CLE-ACSV) (Kim *et al*., 2015), which uses a competitive equilibrium between Zn-complexing ligands naturally present in the sample and a competing ligand (ammonium 1-pyrrolidinedithiocarbamate; APDC) (see Supplementary Materials for theory of Zn speciation analysis). Briefly, a ligand titration consisting of 9 Teflon vials (Savillex) was set up. In each vial, 10 mL of the seawater sample, 4 mM of borate buffer and a known concentration of Zn (0–9 nM) were added. The first two vials were not spiked with Zn and were used as replicates for the starting point of the titration. After 2 h, 25 μM of APDC was added to each vial. At this APDC concentration, the detection window of the method is approximately from $K'_{ZnL,Zn2+}$ = 10^7 to 10^{12} for a C_L of 1 nM, where $K'_{ZnL,Zn2+}$ is the conditional stability constant of the Zn complex with respect to Zn^{2+} in seawater and C_L is the total ligand concentration, respectively. The APDC was allowed to equilibrate for 12 h. The samples were then transferred to a Teflon cell for the measurement. One example of a titration is shown in Supplementary Fig. S2.

Dissolved sulfide analysis

Dissolved sulfide concentrations were determined onboard by using CSV (Rozan *et al*., 1999). In this method, the voltammetric signal may possibly include the currents from free sulfide ($[H_2S]+[HS^-]+[S^{2-}]$), polysulfides, metal hydrosulfides of Mn, Fe, Co, and Ni, and elemental sulfur (S(0)), but the signals were simply transformed to "dissolved sulfide". In this study, we used a 663 VA stand (Metrohm) interfaced with an IME663 and a μAutolab II (Eco Chemie). Seawater sample (10 mL) was added to a Pyrex glass cell. To prevent the loss of H_2S, samples were not purged with N_2 gas before the analysis. The detection limit, calculated as three times the standard deviation of measurements of the surface seawater in open ocean, was 4.8 nM. The standard solution was produced from $Na_2S{\cdot}9H_2O$ powder onboard the ship. The concentrations of dissolved sulfide in the seawater were calibrated using a standard addition method.

Results and Discussion

Hydrography

Figure 2 and Table 1 show the data obtained in this study. We could not observe anomalies of potential temperature, salinity, or dissolved oxygen in the water column by CTD sensors at the coastal stations near Obama Hot Springs (Stn. A, Stn. B, and Stn. 6). A high and narrow range of salinity (33.478–33.799) indicates that there is little fluvial discharge in this study area (Table 1). In a previous study, hot submarine spring vent waters (70–80°C) were collected by the SCUBA diving sampling at these stations (Takeda, 2018). Compared with the SCUBA diving sampling, it was difficult to collect the samples that were close to hydrothermal endmembers, by using OTE samplers. The hydrographic data indicate that the collected plume waters had been diluted with ambient oxic seawater (Fig. 2C). However, the sulfide data of the collected plume waters still indicated clear signatures of the hydrothermal activity as described below.

Dissolved trace metals and sulfide concentrations

In this study, two dissolved sulfide concentrations (29.2 and 59.4 nM) were detected in the bottom waters at Stn. 6, where sulfide concentration increased toward the bottom (Fig. 2I). Since we observed the fumarolic gas emissions from the seafloor bottom at Stn. 6, the detected sulfide seemed to be derived from the hydrothermal activities, though the hydrothermal fluid was diluted with huge amount of surrounding oxygenated seawater.

The profiles of dissolved trace metals at the bottom of the coastal areas (Stn. A, Stn. B, and Stn. 6), where hydrothermal activity has been reported previously (Takeda, 2018 and reference therein), were different from those at Stn. 5 and Stn. 10. At the coastal areas (Stn. A, Stn. B, and Stn. 6), dissolved Mn and Fe concentrations were generally high and increased at the bottom (Figs. 2D and 2E), whereas dissolved Cu and Zn concentrations were generally decreased just above the bottom (Figs. 2F and 2G). On the other hand, the vertical distributions of trace metals at Stn. 5 and Stn. 10 were relatively constant (Fig. 2). At Stn. 6, where dissolved sulfide concentrations were detected at the bottom, dissolved Mn and Fe concentrations were increased by 34% (from 24.5 nM to 32.8 nM) and 104% (from 4.5 nM to 9.1 nM), respectively, whereas dissolved Cu and Zn concentrations were decreased by 15% (from 2.3 nM to 1.9 nM) and 86% (from 2.9 nM to 0.3 nM), respectively (Fig. 2; Table 1).

The concentration levels of the dissolved trace metals (except for Cu) and the dissolved sulfides in plume waters obtained in this study were four or five orders of magnitude lower than those in vent waters at coastal hydrothermally active areas previously reported, whereas dissolved Cu was in the same range of concentration level as shown in Supplementary Table S2, which might be an interesting feature of Cu at the coastal hydrothermal system.

Zn complexation in the hydrothermal activity area

During the Zn speciation analysis, log $K'_{ZnL,Zn2+}$ and C_L were obtained from two samples at Stn. 6 and three samples at Stn. 10 near the bottom (Table 1). The log $K'_{ZnL,Zn2+}$ of natural ligands in Tachibana Bay ranged from 9.9 to 10.3, which is comparable to the values in previous studies of the coastal areas (Supplementary Table S3).

Table 1. Dissolved trace metals and Zn speciation analysis results with associated hydrographic data obtained in this study

Region	Station	Depth (m)	Potential Temp. (°C)	Salinity (PSU)	Dissolved O_2 (μmol/kg)	Free sulfides (nM)	Mn (nM)	Fe (nM)	Cu (nM)	Zn (nM)	C_L (nM)	log $K'_{ZnL,Zn^{2+}}$	Zn^{2+} (nM)	Zn_{labile} (nM)
Coastal area	A	3	19.30	33.478	238.3	n.d.	35.5	13.0	2.4	2.6				1.9
	(32°43.67′ N, 130°12.21′ E)	6	18.47	33.498	245.0	n.d.	39.3	16.5	2.6	3.1				1.7
	(Bottom depth: 18 m)	8	18.08	33.572	241.8	n.d.	29.2	10.4	2.1	2.2				0.9
		11	17.81	33.613	239.6	n.d.	25.6	7.6	1.9	2.6				0.8
		13	17.64	33.624	234.4	n.d.	26.8	10.0	1.8	1.7				0.6
	B	5	18.65	33.506	242.0	n.d.	27.2	5.6	2.4	2.2				0.5
	(32°43.78′ N, 130°12.16′ E)	10	17.79	33.616	239.4	n.d.	28.1	6.4	2.0	2.5				0.7
	(Bottom depth: 25 m)	14	16.99	33.632	228.2	n.d.	30.2	6.6	2.1	2.5				1.0
		17	16.90	33.631	228.0	n.d.	32.1	7.0	2.4	2.7				1.3
		18	16.83	33.633	228.5	n.d.	33.5	7.4	2.3	1.7				0.7
	6	10	17.94	33.584	237.8	n.d.	26.6	6.0	2.3	2.9				1.2
	(32°43.67′ N, 130°12.15′ E)	12	17.78	33.610	238.6	n.d.	24.5	4.5	2.2	1.0				0.7
	(Bottom depth: 22 m)	15	17.62	33.610	233.3	29.2	31.2	7.9	2.0	0.3	0.9	10.3	0.02	0.1
		17	17.04	33.637	228.6	59.4	32.8	9.1	1.9	0.4	1.4	10.2	0.02	0.1
Away from the coastal area	5	5	18.67	33.488	237.9	n.d.	21.6	1.8	2.0	1.8				0.9
	(32°43.73′ N, 130°11.52′ E)	10	18.29	33.549	241.7	n.d.	21.7	3.0	2.0	1.5				0.9
	(Bottom depth: 35 m)	20	17.20	33.628	232.1	n.d.	19.6	2.3	2.3	1.4				0.8
		25	16.93	33.640	226.4	n.d.	25.8	3.1	2.0	1.6				0.9
		31	16.08	33.649	212.1	n.d.	30.3	3.9	2.1	2.2				1.0
Center of the Tachibana Bay	10	5	18.95	33.531	234.8	n.d.	21.2	2.9	2.2	1.5				0.9
	(32°43.23′ N, 130°05.49′ E)	10	17.89	33.676	233.4	n.d.	17.4	2.9	2.0	1.3	1.5	10.0	0.17	0.5
	(Bottom depth: 40 m)	20	17.43	33.799	218.8	n.d.	13.3	2.5	1.8	1.4				0.6
		30	17.29	33.774	215.1	n.d.	20.6	3.4	1.9	1.1	1.6	9.9	0.12	0.4
		36	16.61	33.716	205.9	n.d.	26.6	4.5	2.1	1.4	1.6	10.0	0.16	0.6

n.d. = not detected.

On the other hand, the C_L in Tachibana Bay ranged from 0.9 nM to 1.6 nM, which is one or two orders of magnitude lower than the values at other coastal areas. Previous studies have shown higher dissolved Zn concentrations and C_L in other coastal areas (Supplementary Table S3). The relatively low dissolved Zn and C_L in Tachibana Bay probably occur because there is little fluvial discharge, which could transport both high dissolved Zn and its complexing organic ligands (Kim *et al*., 2015). We did not observe an increase of C_L near the hydrothermal sources, which had a concentration range similar to those in the non-hydrothermal area (Stn. 10) (Table 1). It would imply that those Zn complexing ligands in this study area are derived from ambient seawater. Based on dissolved Zn and labile Zn concentrations during the titrations, at the coastal hydrothermal area (Stn. 6), a slightly larger fraction of dissolved Zn was complexed with organic ligands (93–95%), whereas at the center of the Tachibana Bay (non-hydrothermal area, Stn. 10), the fraction was 88–89%.

The Zn titration, except for the samples from Stn. 6 (n = 2) and Stn. 10 (n = 3), showed a linear increase with added Zn^{2+}. This occurred because the CLE-ACSV technique only enables ligand detection when ligand concentrations exceed dissolved Zn concentrations. To understand the Zn speciation in the Zn-saturated waters, by using same conditions as those of the titration (pH 8.2, addition of 25 μM APDC, 12 h equilibration time), Zn_{labile} was determined in the natural samples without adding Zn and with no UV-irradiation (Fig. 2H). In this study, Zn_{labile} includes not only Zn^{2+} and inorganic Zn, but also the portion of Zn weakly complexed with ligands. The vertical distributions of Zn_{labile} at the coastal areas (Stn. A, Stn. B, and Stn. 6) showed that Zn_{labile} was decreased at the bottom of the distributions, whereas the vertical distributions at Stn. 5 and Stn. 10 were relatively consistent (Fig. 2H), similar to those of dissolved Zn.

Role of Zn complexing ligands in the shallow hydrothermal area

Although previous studies at buoyant hydrothermal vents in the deep open ocean reported that a large portion of Zn was rapidly precipitated onto the seafloor through the formation of ZnS (e.g., German *et al*., 1991), a recent study suggests that mantle-derived Zn from hydrothermal vents could be a net source of dissolved Zn to the deep sea (Roshan *et al*., 2016). In our study, a decrease of dissolved Zn was observed, which might suggest a unique feature of dissolved Zn in this shallow hydrothermal activity area. Our Zn speciation results in this area showed that Zn remained in the dissolved phase and that the dissolved Zn was complexed with organic ligands. Furthermore, Zn_{labile} data (Fig. 2H; Table 1) indicate that certain portion of dissolved Zn might be complexed with organic ligands even though most of samples were already saturated with Zn. Because organic complexation and sulfide precipitation are competing reactions, we evaluated the role of Zn complexing ligands in this shallow hydrothermal activity area.

Assuming that there was no hydrothermal activity at Stn. 6, the dissolved Zn concentrations there in the near surface and at the bottom (only 7 m depth difference) would be identical, and the dissolved Zn concentration at the bottom could therefore be estimated as about 2.9 nM. In the hydrothermal system, seawater is first intruded, (bio)geochemical reactions occur within the geothermal reservoir, and recharged seawater is finally discharged at the surface of the bottom sediment (Saibi and Ehara, 2010) (Fig. 1). We found that concentration of dissolved Zn was 0.4 nM in the bottom waters at Stn. 6. Therefore, most of the Zn was probably removed as ZnS precipitated by hydrothermal activity. Here, assuming that dissolved Zn was removed through the formation of ZnS (2.5 nM), we evaluated the possible concentration level of free sulfide ($[H_2S]+[HS^-]+[S^{2-}]$) based on the concentration of dissolved Zn ion (Zn^{2+}) from the Zn speciation analysis (21 pM). The free sulfide concentrations could be calculated simply by using the solubility of ZnS ($Zn^{2+} + S^{2-} \rightleftarrows ZnS_{(s)}$; $\log K_s = -24.37 \pm 0.24$) (Dyrssen, 1988). In this calculation, $[S^{2-}]$ can be estimated as $1.2–3.5 \times 10^{-14}$ M. By calculating the fractions of free sulfide ($[H_2S]+[HS^-]+[S^{2-}]$) at pH 8.2 using the dissociation constants of hydrogen sulfide (Al-Farawati and van den Berg, 1999), the free sulfide concentration at Stn. 6 can be calculated as 3.0–9.1 nM.

In the areas of hydrothermal activity, other metals, in addition to Zn, such as Hg, Fe, and Cu, could form metal sulfides and precipitate onto the seafloor (e.g., German *et al*., 1991). Among other metals, Hg has the highest stability constant ($K'_{HgS} = [HgS]/[Hg^{2+}][S^{2-}] = 10^{42.0}$) compared to ZnS ($K'_{ZnS} = [ZnS]/[Zn^{2+}][S^{2-}] = 10^{18.5}$) (Dyrssen, 1988). A previous study in the Kagoshima Bay, where shallow coastal hydrothermal activity has been reported, total Hg concentrations in seawater samples were in the range of 0.24–15.2 pM (Tomiyasu *et al*., 2015). Even if all the Hg were available for sulfide formation, the HgS fraction would be negligible for total sulfide concentrations. CuS ($K'_{CuS} = [CuS]/[Cu^{2+}][S^{2-}] = 10^{26.0}$) is also more stable thermodynamically than ZnS by seven orders of magnitude (Dyrssen, 1988). A previous Cu speciation study in the shallow non-buoyant coastal hydrothermal activity areas (Milos, Dominica, and the Bay of Plenty) reported $\log K'_{CuL,Cu2+}$ values of 11.6–14.0 and C_L values of 2.1–56.8 nM (Kleint *et al*., 2015). Because we did not analyze Cu speciation in this study, we estimated the competition for Cu speciation between organic ligand and sulfide by using the organic ligand data for Cu at the surface (10 m) of the East China Sea (log

$K'_{CuL,Cu2+}$ of 13.3, C_L of 8.3 nM) (Wong *et al*., 2018). Assuming $[S^{2-}]$ as $1.2–3.5 \times 10^{-14}$ M and the dissolved Cu concentration as 2.26 nM, organic complexed Cu was calculated as $1.1–3.2 \times 10^{-16}$ M, which indicates that most of the dissolved Cu (>99%) would form CuS. However, dissolved Cu concentrations were decreased by only 15% (from 2.3 nM to 1.9 nM) at Stn. 6, whereas dissolved Zn was decreased sharply (from 2.9 nM to 0.3 nM) (Figs. 2F and 2G).

The calculation implies that a large fraction of the dissolved Cu could be derived via the re-dissolution of particulate CuS. A study in areas of hydrothermal activity in the deep open ocean (Mid-Atlantic Ridge) reported the oxidative re-dissolution of CuS particles in the transition zone between suboxic and oxic waters (Sarradin *et al*., 2009). Then, this dissolved Cu, released from CuS, would be complexed with organic ligands, as suggested by Sander and Koschinsky (2011). This process could be a reason for the only 15% decrease of dissolved Cu, while 86% of the Zn was removed through the formation of ZnS, which persists stably in the transition zone between suboxic and oxic waters in hydrothermally active areas (Sarradin *et al*., 2009 and reference therein).

At Stn. 6, dissolved sulfides were detected, but the calculated free sulfide concentration from the Zn speciation was much lower than the measured values. As mentioned previously, for dissolved sulfide determination, the voltammetric signal includes the currents from not only free sulfide ($[H_2S]+[HS^-]+[S^{2-}]$) but also from polysulfides, metal hydrosulfides of Mn, Fe, Co, and Ni, and S(0) (Rozan *et al*., 1999). In seawater at pH ≥ 7, complexes of Mn, Fe, Co, and Ni with hydrosulfide could be present in dissolved phase as labile hydrosulfide species ($\log K'_{Metal\text{-}HS}$ = 4.6–5.1), while complexes of Zn and Cu are present as ZnS and CuS (Luther *et al*., 1996). In this study, we estimated that very low concentrations of hydrosulfides of Zn ($1.9–5.9 \times 10^{-13}$ M) and Cu (7.2×10^{-16} M) would be present due to the high conditional stability constants of ZnS ($\log K'_{ZnS}$ = 18.5) and CuS ($\log K'_{CuS}$ = 26.0) compared to those of the hydrosulfides of Zn and Cu ($\log K'_{Metal\text{-}HS}$ = 6.5 and 14.1, respectively) (Dyrssen, 1988). Furthermore, even though Mn, Fe, Co, and Ni can be complexed with hydrosulfide, the concentrations of these metal hydrosulfides might be negligible due to their low conditional stability constants ($\log K'_{Metal\text{-}HS}$ = 4.6–5.1) (Luther *et al*., 1996), which result in low concentrations of the metal hydrosulfides in seawater (e.g., Fe hydrosulfide would be present at a concentration level of $10^{-11}–10^{-12}$ M even when assuming that all dissolved Fe is Fe^{2+}).

In oxic seawater, dissolved sulfur can be present as S(0). During the oxidation of sulfide, polysulfides can form as intermediate species and then quickly react with excess Fe to form FeS and S(0). A recent study of buoyant hydrothermal vents along the Mid-Atlantic Ridge, also suggested that S(0) is a significant component (5–85%) during the sulfide oxidation via an Fe catalytic cycle (Findlay *et al*., 2014 and reference therein). In this study, dissolved Fe was enriched at the bottom in the coastal areas (Stn. A, Stn. B, and Stn. 6) (Fig. 2E). The signal detected by CSV may have included reduction currents from S(0) present in this hydrothermal system.

Because dissolved Zn and its organic complexation have not been studied in a hydrothermal system, this study provides a first approach to understanding the organic Zn complexation of a coastal hydrothermal system. However, because of the limited dataset, it remains unclear how Zn could remain in the dissolved phase. Additional Zn speciation studies including the particulate phase are needed to clarify the relevant mechanisms in the hydrothermal area.

At the buoyant hydrothermal vents in the deep open ocean, hydrothermal fluids with dissolved sulfide concentrations that may be in the μM range are discharged to deep waters (Findlay *et al*., 2014; Kleint *et al*., 2016). Furthermore, it has been reported that the dissolved Fe concentrations and their C_L in these systems are very high compared to those of non-buoyant shallow hydrothermal activity areas (Kleint *et al*., 2016). Previous studies in buoyant hydrothermal activity areas of the deep open ocean have also reported increases of dissolved Zn near the hydrothermal plumes (Roshan *et al*., 2016), which is opposite to our study in this unique shallow hydrothermal activity area, where a decrease of dissolved Zn has been observed. Therefore, the (bio)geochemical cycles of dissolved Zn may be different among hydrothermally active areas, depending on the geological setting. In buoyant hydrothermal activity areas of the deep open ocean, excess dissolved Zn may exist due to the formation of Zn-sulfide nanoparticles in hydrothermal plumes, as suggested for dissolved Fe and Cu (Sands *et al*., 2012 and reference therein). Furthermore, if Zn is stabilized by organic ligands, it may persist in dissolved phase. However, there are only a few studies of Zn complexation in deep waters, which did not show any strong evidence for organic Zn complexation at depth (e.g., Ellwood and van den Berg, 2000). Moreover, we could not find any information about Zn complexing ligands in the hydrothermal activity areas of the deep ocean. Therefore, this remains purely speculative until it is demonstrated. Nonetheless, the Zn complexing ligands in hydrothermal activity areas might provide insights into the dissolved Zn in hydrothermally active environments.

Conclusion

In this study, we determined the dissolved trace metal concentrations, Zn speciation, and dissolved sulfide at a

shallow coastal hydrothermal area, Tachibana Bay. In the central area of the bay, all the metals including Mn, Fe, Cu, and Zn showed the same feature, but near the hydrothermally active area, dissolved Mn and Fe concentrations increased toward the bottom, whereas dissolved Cu and Zn concentrations decreased, which might indicate that geochemical reactions vary depending on the trace metal elements near the hydrothermal sources.

Our Zn speciation data, which are the first data obtained at a shallow hydrothermally active area, as far as we are aware, clearly showed that organic complexed Zn can be present in dissolved phase. Although dissolved Zn distributions in areas of hydrothermal activity may vary from site to site depending on the site-specific conditions, this result might suggest that organic complexing ligands play an important role in the presence of dissolved Zn in hydrothermal activity areas. Further research will clarify the processes by which Zn complexing ligands can hold Zn in the dissolved phase in other hydrothermal areas.

Acknowledgments—This study was supported by Grants-in-Aid for Scientific Research (A) (Nos. 23253001 and 16H02701) and Grants-in-Aid for Scientific Research in Innovative Areas "Ocean Mixing Processes" (No. JPH05820) from Monkasho (Ministry of Education, Culture, Sports, Science and Technology: MEXT). We thank all the crews and participants of the cruise on the TS *Kakuyo-maru*. We are thankful to the anonymous reviewers for their useful comments that helped to improve the manuscript.

HIGHLIGHTS

- This study explores organic Zn complexation in a shallow coastal hydrothermal area.
- Dissolved Zn and Cu decrease in bottom waters near the hydrothermally active area.
- Organic ligands may play an important role for dissolved Zn in some hydrothermal areas.

REFERENCES

Al-Farawati, R. and van den Berg, C. M. G. (1999) Metal-sulfide complexation in seawater. *Mar. Chem.* **63**, 331–352. doi:10.1016/S0304-4203(98)00056-5.

Dyrssen, D. (1988) Sulfide complexation in surface seawater. *Mar. Chem.* **24**, 143–153. doi:10.1016/0304-4203(88)90045-X.

Ellwood, M. J. and van den Berg, C. M. G. (2000) Zinc speciation in the Northeastern Atlantic Ocean. *Mar. Chem.* **68**, 295–306. doi:10.1016/S0304-4203(99)00085-7.

Findlay, A. J., Gartman, A., MacDonald, D. J., Hanson, T. E., Shaw, T. J. and Luther, G. W., III (2014) Distribution and size fractionation of elemental sulfur in aqueous environments: The Chesapeake Bay and Mid-Atlantic Ridge. *Geochim. Cosmochim. Acta* **142**, 334–348. doi:10.1016/j.gca.2014.07.032.

Fitzsimmons, J. N., John, S. G., Marsay, C. M., Hoffman, C. L., Nicholas, S. L., Toner, B. M., German, C. R. and Sherrell, R. M. (2017) Iron persistence in a distal hydrothermal plume supported by dissolved-particulate exchange. *Nat. Geosci.* **10**, 195–201. doi:10.1038/ngeo2900.

German, C. R., Campbell, A. C. and Edmond, J. M. (1991) Hydrothermal scavenging at the Mid-Atlantic Ridge: Modification of trace element dissolved fluxes. *Earth Planet. Sci. Lett.* **107**, 101–114. doi:10.1016/0012-821X(91)90047-L.

Kim, T., Obata, H., Kondo, Y., Ogawa, H. and Gamo, T. (2015) Distribution and speciation of dissolved zinc in the western North Pacific and its adjacent seas. *Mar. Chem.* **173**, 330–341. doi:10.1016/j.marchem.2014.10.016.

Kleint, C., Kuzmanovski, S., Powell, Z., Bühring, S. I., Sander, S. G. and Koschinsky, A. (2015) Organic Cu-complexation at the shallow marine hydrothermal vent fields off the coast of Milos (Greece), Dominica (Lesser Antilles) and the Bay of Plenty (New Zealand). *Mar. Chem.* **173**, 244–252. doi:10.1016/j.marchem.2014.10.012.

Kleint, C., Hawkes, J. A., Sander, S. G. and Koschinsky, A. (2016) Voltammetric investigation of hydrothermal iron speciation. *Frontiers Mar. Sci.* **3**, 75. doi:10.3389/fmars.2016.00075.

Kondo, Y., Obata, H., Hioki, N., Ooki, A., Nishino, S., Kikuchi, T. and Kuma, K. (2016) Transport of trace metals (Mn, Fe, Ni, Zn and Cd) in the western Arctic Ocean (Chukchi Sea and Canada Basin) in late summer 2012. *Deep-Sea Res. Part I: Oceanographic Research Papers* **116**, 236–252. doi:10.1016/j.dsr.2016.08.010.

Luther, G. W., III, Rickard, D. T., Theberge, S. and Olroyd, A. (1996) Determination of metal (bi)sulfide stability constants of Mn^{2+}, Fe^{2+}, Co^{2+}, Ni^{2+}, Cu^{2+}, and Zn^{2+} by voltammetric methods. *Environ. Sci. Technol.* **30**, 671–679. doi:10.1021/es950417i.

Morel, F. M. M. and Price, N. M. (2003) The biogeochemical cycles of trace metals in the oceans. *Science* **300**, 944–947. doi:10.1126/science.1083545.

Roshan, S., Wu, J. and Jenkins, W. J. (2016) Long-range transport of hydrothermal dissolved Zn in the tropical South Pacific. *Mar. Chem.* **183**, 25–32. doi:10.1016/j.marchem.2016.05.005.

Rozan, T. F., Benoit, G. and Luther, G. W., III (1999) Measuring metal sulfide complexes in oxic river waters with square wave voltammetry. *Environ. Sci. Technol.* **33**, 3021–3026. doi:10.1021/es981206r.

Saibi, H. and Ehara, S. (2010) Temperature and chemical changes in the fluids of the Obama geothermal field (SW Japan) in response to field utilization. *Geothermics* **39**, 228–241. doi:10.1016/j.geothermics.2010.06.005.

Sander, S. G. and Koschinsky, A. (2011) Metal flux from hydrothermal vents increased by organic complexation. *Nat. Geosci.* **4**, 145–150. doi:10.1038/ngeo1088.

Sands, C. M., Connelly, D. P., Statham, P. J. and German, C. R. (2012) Size fractionation of trace metals in the Edmond hydrothermal plume, Central Indian Ocean. *Earth Planet. Sci. Lett.* **319–320**, 15–22. doi:10.1016/j.epsl.2011.12.031.

Sarradin, P.-M., Waeles, M., Bernagout, S., Le Gall, C.,

Sarrazin, J. and Riso, R. (2009) Speciation of dissolved copper within an active hydrothermal edifice on the Lucky Strike vent field (MAR, 37°N). *Sci. Total Environ.* **407**, 869–878. doi:10.1016/j.scitotenv.2008.09.056.

Takeda, S. (2018) Shallow submarine hydrothermal system in Tachibana Bay, Nagasaki, Japan—II: Chemical characteristics of submarine hot spring water. *Bull. Fac. Fisheries, Nagasaki Univ.* **99**, 1–6 (in Japanese with English abstract and figures).

Tomiyasu, T., Minato, T., Ruiz, W. L. G., Kodamatani, H., Kono, Y., Hidaka, M., Oki, K., Kanzaki, R., Taniguchi, Y. and Matsuyama, A. (2015) Influence of submarine fumaroles on the seasonal changes in mercury species in the waters of Kagoshima Bay, Japan. *Mar. Chem.* **177**, 763–771. doi:10.1016/j.marchem.2015.10.009.

Wong, K. H., Obata, H., Kim, T., Wakuta, Y. and Takeda, S. (2018) Distribution and speciation of copper and its relationship with FDOM in the East China Sea. *Limnol. Oceanogr.* (submitted).

Supplementary Materials

URL (http://www.terrapub.co.jp/journals/GJ/archives/data/52/MS545.pdf)
Figures S1 and S2
Tables S1 to S3